PAPER

Promising Developments in Marine Applications With Artificial Muscles: Electrodeless Artificial Cilia Microfibers

AUTHORS

Kwang J. Kim
Viljar Palmre
Tyler Stalbaum
Taeseon Hwang
Qi Shen
Sarah Trabia
Active Materials and Smart Living Laboratory, Department of Mechanical Engineering, University of Nevada, Las Vegas

ABSTRACT

Ionic polymer-metal composite artificial muscles have received great research attention in the development of robotic manipulators, advanced medical devices, and underwater propulsors, such as artificial fish fins. This is due to their unique properties of large deformation, fast dynamic response, low-power requirements, and the ability to operate in aquatic environments. Recently, locomotion of biological cells and microorganisms through unique motion of cilium (flagellum) has received great interest in the field of biomimetic robotics. It is envisioned that artificial cilia can be an effective strategy for maneuvering and sensing in small-scale bioinspired robotic systems. However, current actuators used for driving the robots are typically rigid, bulky in mechanism and electronics requirements producing some acoustic signatures, and difficult to miniaturize. Herein, we report biomimetic, wirelessly driven, electroactive polymer (EAP) microfibers that actuate in an aqueous medium when subjected to an external electric field of <5 V/mm, which can be realized to create cilia-based robotic systems for aquatic applications. Initial development and manufacturing of these systems is presented in this paper. The EAP fibers are fabricated from ionic polymer precursor resin through melt-drawing process and have a circular cross-section with a diameter of 30–70 μm. When properly activated and subjected to an electric field with switching polarity, the EAP fibers exhibit cyclic actuation with adequate response time (0.05–5 Hz). The experimental results are presented and discussed to demonstrate the performance and feasibility of biomimetic cilia-based microactuators. Prospective bioinspired applications of the artificial muscle cilia-based system in marine operations are also discussed.

Keywords: artificial muscles, ionic polymer-metal composite, electroactive fibers, artificial cilia array

Introduction

Many aquatic life forms are equipped with natural tools for high maneuverability, environmental sensing, and capturing or escaping from target or prey, respectively. These characteristics improve survival and well-being in often harsh or predatory-rich environments. The employed mechanisms are commonly unique to a select few natural creatures, which attributes to the survival of very different species in the same environments. Researchers have long aspired to mimic these natural traits by designing robotic mechanisms and advanced materials to create new technologies in marine operations (Ball, 1999, 2001, 2002; Bar-Cohen, 2006; Shahinpoor & Kim, 2004a, 2004b; Bhushan, 2009; Bandyopadhyay et al., 2008). Examples of these developments include robotic devices such as artificial muscles (AMs), fish-fin-like underwater propulsors, full bioinspired underwater vehicle designs, and even intricately structured, soft, artificial skin substrates (Deng & Avadhanula, 2005; Zhou & Low, 2012; Yu et al., 2004; Fish et al., 2008; Kamamichi et al., 2006; Kim et al., 2005, 2007, 2011; Palmre et al., 2012; Yim et al, 2007; Shen et al., 2013; Guo et al., 2006, 2007; Najem et al., 2012; Lauder & Madden, 2007; Ball, 1999; Wen et al., 2014).

One such natural system that has been investigated for prospective biomimetic marine applications is cilia and flagella of mammalian cells for microflow control and microlocomotion mechanisms (Zhou & Liu, 2008; Oh et al., 2009; den Toonder & Onck, 2013). Cilia and flagella are microtubular protrusions from the surface of many eukaryotic cells and are of two main types: motile, those capable of moving independently, and nonmotile cilia (Satir & Christensen, 2007, 2008). They are found in cells in nature and play a critical role in health and well-being, often functioning as mechanisms to move cells or

objects through a flow channel, such as in the case of human windpipe, brain ventricles, and Fallopian tubes, as examples (Enuka et al., 2012), in case of motile cilia. Nonmotile cilia, found in many cells in nature, typically operate as a sensory system. However, motile cilia and nonmotile cilia are structurally similar, and both can function as signaling devices (Satir & Christensen, 2007, 2008). As sensory organelles, these transfer information of extracellular signals to control several cellular processes (Satir & Christensen, 2007). Thus, sensory information from cilia is thought to be coupled to motile cilia for feedback environmental sensing and control (Satir & Christensen, 2007, 2008). These characteristics have made cilia organelles a promising candidate for bioinspired device development in microfluidics and marine operations. The prospective applications of a simple, surface-mountable microartificial cilia environmental sensory and control system range from near-surface flow control of underwater vehicles to advanced medical operations in drug delivery systems.

This paper exploits the unique properties of an in-lab designed AM microtransducer to develop a working cilia-based microactuator array for marine applications. An AM is a multifunctional, smart polymer whose electromechanical properties can be controlled, resulting in reproducible actuation and sensing capabilities (Shahinpoor & Kim, 2001; Kim & Shahinpoor, 2003; Shahinpoor & Kim, 2004b). Like biological muscles, the AM technology exhibits large motion, good force, fast response, good efficiency, long cycle life, and silent operation. Recent research on the locomotion of biological cells and microorganisms has identified the importance of cilium (flagellum) and its unique motion for propulsion and maneuvering (Satir & Christensen, 2007, 2008). However, recent man-made attempts at mimicking the motion of cilium using traditional actuators have yielded limited success, and often the designs are bulky (Zhou & Liu, 2008; Oh et al., 2009; den Toonder & Onck, 2013). On the contrary, the AM technology is an excellent candidate for realizing the complex oscillatory motion of cilium for the development of efficient and highly maneuverable underwater actuator and sensor systems for marine applications.

The current state-of-the-art AM technology is limited to creating thin strips or cantilever-style actuators due primarily to difficulties associated with material processing. Recent advances in AM materials processing work and research have resulted in AMs that can produce forces on the order of tens of gram-force for a standard sample of 1-cm wide by 5-cm long by 1-mm thick. However, the manufacturing of slender rod-like AMs with sectored electrodes has been challenging (Kim et al., 2015). Additionally, these devices require two or more separated electrodes per sample to actuate. Herein, the authors report a new electrodeless electroactive polymer (EAP) microactuator that actuates wirelessly by low external electric field and is capable of AM maneuverability. It is an ionic type EAP actuator with no built-in surface electrode layers. The new electrodeless EAP actuator consists of only one single perfluorinated EAP material. Due to its simple structure, the electrodeless EAP actuators are simple to fabricate into a variety of shapes and can be easily miniaturized to microscale, which is needed for the development of small bioinspired robotic systems such as artificial cilia or flagella. Our group has successfully demonstrated fabrication of AM with different geometries, including rod-shaped AMs that can undergo bending actuation and sensing in multiple directions and microactuator fibers that have been expanded into prototype AM cilia arrays (1 × 20).

AM Fibers

Ionic polymer-metal composite (IPMC) transducers, made from an ionomer-based EAP, which have been used successfully as 3D microsensors in previous works (Feng & Tsai, 2011; Stalbaum et al., 2015), are a strong motivation for this study for development into the cilia-like AM microactuator array due to their unique and well-suited properties. These devices exhibit fast dynamic response, high spatial resolution, and low electronics and mechanisms requirements and are best suited for operation in aqueous environments (Shahinpoor & Kim, 2001; Kim & Shahinpoor, 2003). Additionally, they are silent in operation, are low in power consumption, and can be designed to operate in different fluid environments (Bar-Cohen, 2004). Furthermore, they can operate as actuators or sensors (Alici et al., 2008, Pugal et al., 2010) and have been designed into self-sensing actuators (Punning et al., 2007; Kruusamäe et al., 2010; Ko et al., 2009). These characteristics make this type of AM a good material candidate for this research with a strong existing technical groundwork. However, IPMC electrode plating is a cumbersome process, and these devices require separated electrodes per sample to actuate.

Conventionally, IPMC material consists of an ionic polymer membrane, typically Nafion material, chemically plated on both surfaces with conductive metal layers, typically

of Pt or Au, that serve as conductive electrodes. To enable an electroactive capability, the ionomer membrane is solvated with an electrolyte, typically Li^+ or Na^+ ions in water solution. When a DC voltage (<5 V) is applied to the electrodes, the hydrated cations migrate toward the negatively charged electrode, leading to internal pressure change, which, in turn, causes a bending of the IPMC toward the positive electrode. The electromechanical performance of an IPMC is highly dependent on the electrical conductivity, flexibility, and surface morphology of the electrodes (Shahinpoor & Kim, 2000; Shen et al., 2014, 2015). The electrode structure determines the adsorption of electrolyte ions at the electrode interface (accumulated charge) that is directly proportional to the electromehanical deformation of the material. As such, the electrodes have many critical design requirements that pose several engineering challenges in terms of performance, manufacturing, and scalability. Also, due to the presence of electric potential and liquid electrolytes, the choice of suitable electrode materials is restricted to electrochemically stable (inert) materials. Therefore, noble metals (such as Pt or Au), carbon nanotubes, carbide-derived carbons, and other carbon derivatives are used for electrodes.

Herein, the authors report a new AM for biomimetic applications, an electrodeless EAP microactuator that actuates wirelessly by low external electric field (<5 V/mm). It is an ionic type EAP actuator similar to the IPMC but with no built-in surface electrode layers. Hence, it is simply called an EAP actuator. As opposed to traditional trilayer IPMC actuators with surface electrodes that comprise different materials and require complex manufacturing processes, the new electrodeless EAP actuator consists of only one single perfluorinated EAP material. Due to its simple structure, the electrodeless EAP actuators are simple to fabricate into variety of shapes and can be easily miniaturized to microscale, which is needed for the development of small bioinspired robotic systems such as artificial cilia (or flagellum). It is envisaged that artificial cilia can be an effective strategy for locomotion and maneuvering of next-generation miniature underwater robotic and microfluidic systems (Zhang et al., 2006; Edd et al., 2003). However, the existing smart actuator technologies face challenges in downscaling to microscale due to their complex structure and manufacturing process and electrical conductivity issues related to miniaturizing the surface electrodes. For instance, down-scaling a trilayered polymeric composite actuator requires much thinner and more flexible electrodes than in case of metallic Pt or Au electrodes and can become problematic due to loss in mechanical robustness, which is required to maintain electrical conductivity and durability.

To demonstrate the feasibility of our new electrodeless EAP fiber microactuators for small-scale bioinspired robotic applications, an AM cilia fiber array system is developed. The electrodeless fiber EAP microactuators are fabricated from a perfluorinated precursor resin of Nafion through melt-drawing process. By careful control of the drawing conditions, cylindrical fibers with a diameter size down to 30 μm are successfully produced. These microfibers, when converted to electroactive form by a simple chemical treatment and subjected to an aqueous medium, display controllable electromechanical actuation in response to low external electric field (<5 V/mm). The prototype cilia array is capable of different aquatic motions such as flapping, bending, and oscillation when driven wirelessly by different external electric fields.

Fabrication of Cilium-Inspired, Electroactive Fibers

The electroactive ionomer fibers were fabricated from Nafion precursor resin through a melt-drawing process

FIGURE 1

Fabrication of cylindrical electroactive ionomer fibers by melt-drawing process.

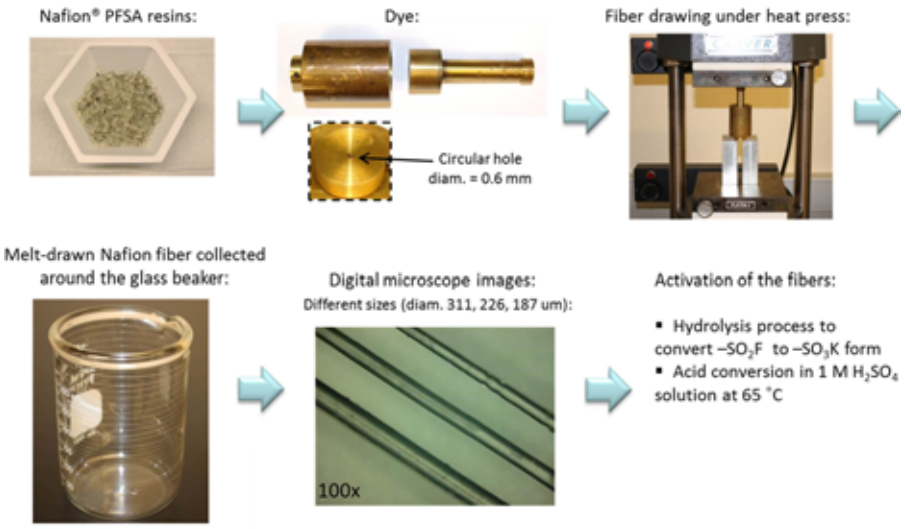

(Figure 1). First, the inactive perfluorinated precursor resin in the sulfonyl fluoride ($-SO_2F$) form was placed in a custom-made extruder die and preheated. As a perfluorinated precursor resin, Nafion polymer does not have the ion exchange capability and is thermoplastic and can be easily melt-processed into variety of shapes. The custom extruder die assembly (shown in Figure 1, top center) was preheated to 240°C and slightly pressurized initially to generate polymer flow through the die. Then, the exiting polymer thread was drawn with uniform speed and collected around a rotating glass drum. Compared to conventional fiber extrusion, the drawing process significantly reduces the diameter size of the fiber as it exits from a die and induces the molecular orientation of polymer chains, increasing the degree of crystallinity and tensile strength of the fiber. Fibers with different dimensions were created by varying the drawing speed and collector drum distance from the die.

The obtained cylindrical Nafion fibers had to be activated by a chemical treatment to enable the cation exchange capability. Table 1 describes the activation process by which the Nafion precursor was converted to "active" sulfonic acid ($-SO_3H$) form. The first step was the hydrolysis process in hot aqueous potassium hydroxide (KOH) and dimethyl sulfoxide (DMSO) for 1 h to convert the ($-SO_2F$) functional groups into sulfonate groups ($-SO_3K$). Next, the polymer was converted to sulfonic acid ($-SO_3H$) form by treatment in a bath of H_2SO_4 solution. Finally, the polymer fibers were cleaned in deionized (DI) water to remove the acid residues.

FIGURE 2

Experimental setup used for measuring the displacement of electroactive ionomer fiber under external electric field.

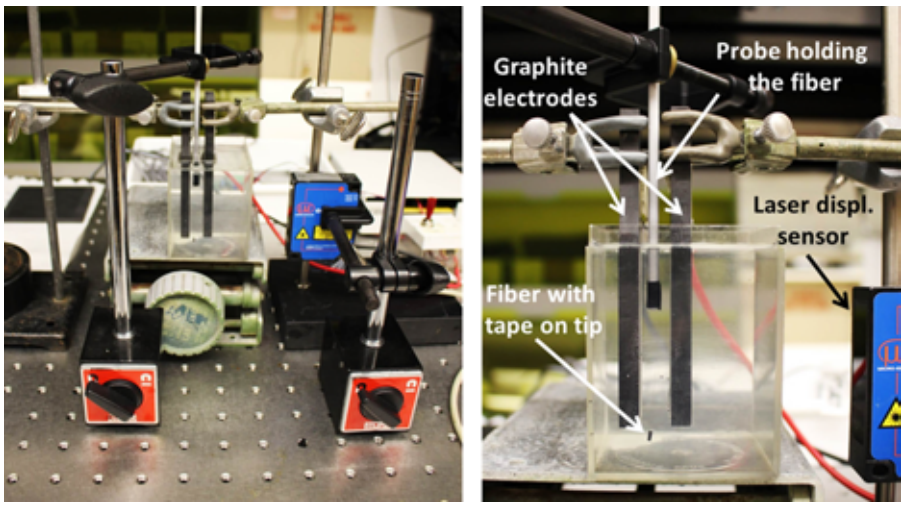

Experimental Methods

A cylindrical Nafion fiber fabricated by melt-drawing process was suspended in 0.1 M LiCl aq. solution between two parallel graphite electrode plates (Figure 2). The distance between the electrodes was 10 mm, and the effective length of the fiber was 42 mm. The bottom end of the fiber reached slightly lower than the electrodes to allow access to the laser beam for displacement measurement. A small piece of tape was attached to the fiber tip, serving as a target for a laser beam. A laser displacement sensor with National Instruments/LabView DAQ system was used for measuring the fiber tip displacement under AC square-wave input of 5 V at frequencies from 0.1 to 1 Hz.

TABLE 1

Activation process of ionomer cilia fibers.

Procedure		Amount	Temperature	Time
1	Soak in KOH (15%), DMSO (30%)	350 ml	95°C	1 h
2	Soak in H_2SO_4	350 ml	75°C	3 h
3	Soak in DI water	350 ml	75°C	45 min
4	Soak in new DI water	350 ml	75°C	45 min

Results and Discussion

Figure 3 shows the fabricated EAP microfibers in different diameter sizes —32 µm and 55 µm produced by melt-drawing process using a 175-µm and 210-µm diameter die, respectively. The fabricated ionomer fibers have a smooth surface morphology and circular cross-section. The thickness of the melt-drawn fibers is highly dependent on the die size and drawing speed. To downscale the diameter size of the EAP fibers, the die size was significantly reduced. Table 2 shows the size range

FIGURE 3

Digital optical microscope images of the fabricated EAP microfibers in different sizes.

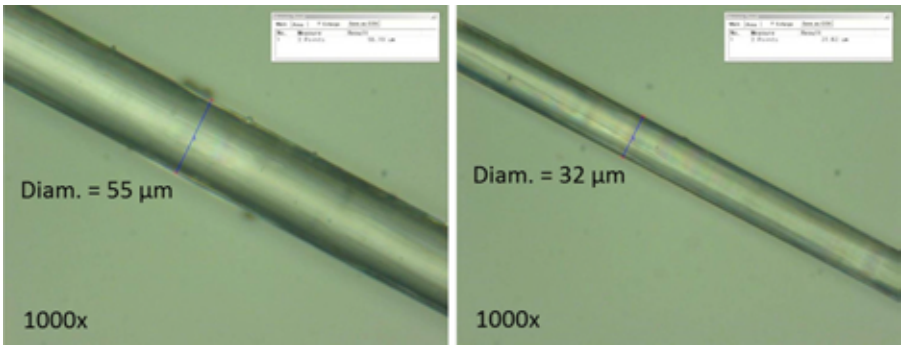

of the fibers produced with different dies. With the smallest 175-µm die, EAP fibers in diameter of 25–45 µm were successfully created.

To demonstrate electromechanical actuation of the new actuators, an individual EAP fiber in cantilever configuration with a free-length of 42 mm was suspended between two graphite electrode plates with a distance of 10 mm and immersed in 0.1 M LiCl aqueous electrolyte solution (Figure 2). The electric field was applied to the (external) graphite plates to wirelessly actuate the fiber. Figure 4 shows the measured voltage and displacement responses in time for the EAP fiber microactuator under an external field of 5 V AC square-wave at 0.1 Hz and 1 Hz. It can be seen that the fiber exhibits repeatable cyclic actuation performance with adequate response. Unlike IPMC actuator that bends toward the positive electrode (anode), the EAP fiber deflects toward the negative electrode (cathode). This can be explained by the fact that Nafion is a cation exchange polymer that can only pass or conduct cations but is nontransparent to anions. Since the Nafion membrane (fiber) does not have a charged electrode boundary at the surface as in case of IPMC with surface electrodes, the cations (Li^+) of the electrolyte migrate through the ionic polymer under the imposed electric field. This results in a cationic current in the polymer that draws the fiber along toward the negative (external) graphite electrode. At the same time, the anionic current of Cl^- ions toward the opposite electrode (anode) has no effect on the fiber as the anions are unable to freely move. Furthermore, the voltage-dependent displacement curves are different than conventional IPMC actuators, as can be observed in the voltage-displacement curve in Figure 5, displaying large hysteresis.

The same experiment was also conducted in ultrapure deionized water (resistivity 18.2 MΩ cm). In this case, the actuation would only rely on Li^+ ions inside the ionomer fiber that balance the fixed anionic functional groups ($-SO_3^-$), which are present due to previous exposure to LiCl electrolyte. However, even at much higher electric fields (>10 V/mm), the fiber exhibited minimal actuation and the response was hesitant. Conducting the experiment in an electrolyte solution (NaCl or LiCl, ≥0.1 M) reduced significantly the required potential and produced much larger/stronger displacement response. Thus, the actuation of EAP fiber is driven by the transport of cations (or cationic current) through the ionomer fiber, as illustrated in Figure 6a. Figure 6b shows the actuation schematic of a conventional IPMC for comparison. In application perspective, actuating the fibers in electrolyte salt solutions would be very convenient as the EAP fibers are intended for use in underwater applications where typical salinity of seawater is ~0.5–0.6 M (NaCl). Therefore, the prepared EAP fibers would be further investigated in marine environment (NaCl solution) in the future.

Preliminary 2D finite element physics-based modeling in COMSOL® Multiphysics 5.2 of a Nafion EAP fiber immersed in a 0.1-M LiCl solution was performed based on the physics discussed above. The results show good agreement for fiber tip displacement using governing physics as shown in Figure 6b as a simplified illustration, using the Poisson-Nernst-Planck equations for diffusion

TABLE 2

Die sizes used for downscaling the size of cylindrical EAP fibers.

Die diameter size (µm)	Fiber diameter range (µm)
610	200–300
310	70–100
210	30–55
175	25–45

FIGURE 4

Applied voltage and measured displacement response of a cylindrical EAP fiber microactuator at 5-V AC square-wave at 0.1-Hz (left) and 1-Hz (right) operating frequencies in 0.1-M LiCl aq. solution at 10-mm electrode spacing.

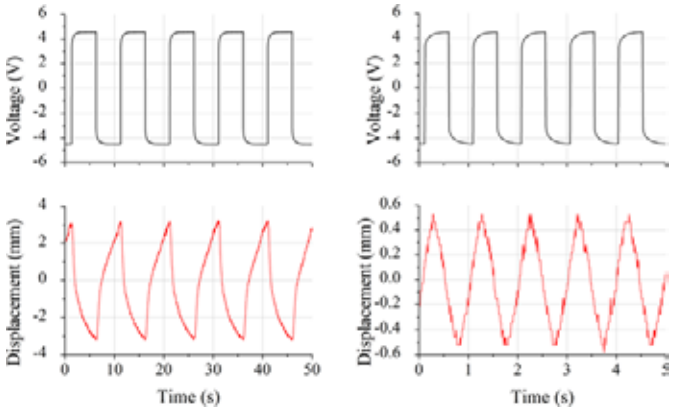

and charge density within the polymer membrane and primary current distribution physics for the electrolyte solution. The primary difference to modeling of conventional IPMC actuators is in the additional electrolyte physics, utilizing the primary current distribution physics module. Additionally, there are no electrodes or electric current physics at the Nafion fiber surface. The electrodes are instead 100 mm^2 surface area electrodes separated by 10 mm to correspond with experimental data of Figure 4. Utilizing the Nernst-Planck (1a) and Poisson's (1b) equations as follows:

$$\frac{\partial c}{\partial t} + \nabla \cdot (-D\nabla C - z\mu FC\nabla\phi) = 0 \quad (1a)$$

$$-\nabla^2\phi = \frac{\rho}{\varepsilon} = \frac{F(C - C_a)}{\varepsilon} \quad (1b)$$

where C is the cation concentration in the polymer membrane, D is the diffusion coefficient of Li^+ ions in the polymer membrane, z is the charge number, F is Faraday's constant, ϕ is electric potential in the polymer membrane, ρ is the charge density, ε is the effective dielectric permittivity value, and C_a is the anion concentration, which is maintained fixed to the polymer backbone. The mobility can be written as $\mu = D/(R \cdot T)$, where R is the gas constant and T is the temperature.

Primary current distribution physics are used in the electrolyte domain. With the equation for electrolyte potential given as

$$-\Delta\phi_l = \frac{Q}{\sigma_e} \quad (2)$$

where ϕ_l is the electrolyte potential, Q is the electrolyte charge, and σ_e is the electrolyte conductivity. A Dirichlet boundary condition is applied at the

FIGURE 5

Displacement response versus applied voltage for a cylindrical EAP fiber microactuator at 5 V AC square-wave at 0.1 Hz operating frequency in 0.1 M LiCl aq. solution at 10 mm electrode spacing.

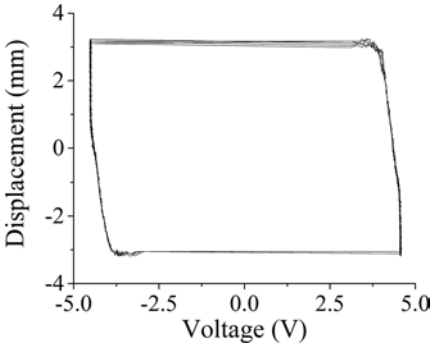

FIGURE 6

Illustration of actuation mechanism of an electrodeless EAP fiber in electrolyte solution under an imposed electric field (a), with a schematic of the actuation mechanisms of a traditional IPMC for contrast (b).

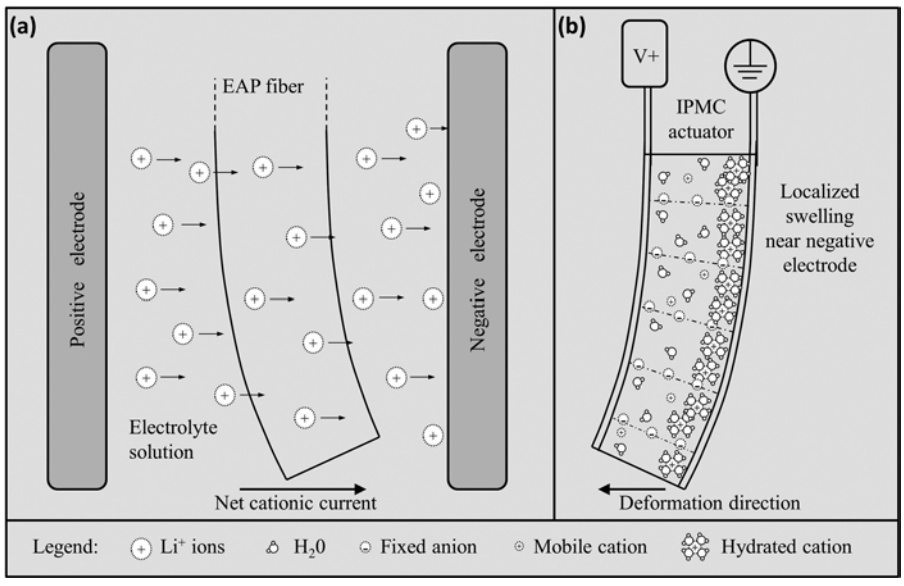

TABLE 3

Parameter values used in COMSOL® Multiphysics simulations.

Parameter	Value
D	7e–11 [m^2/s]
F	96485.3415 [s A/mol]
R	8.31 [J/(mol K)]
T	293 [K]
C_a	1,200 [mol/m^3]
ε	2 [mF/m]
σ_e	3 [mS/cm]
ρ_p	2,000 [kg/m^3]
α	1.5e–7 [V/m]

FIGURE 7

Finite element simulations of an EAP fiber in electrolyte solution as actuated by a 5-V, 1-Hz square wave applied to electrodes spaced 10 mm apart with comparison to experimental results (left) and a close-up of the mesh used for simulations on the free-end of the fiber (right).

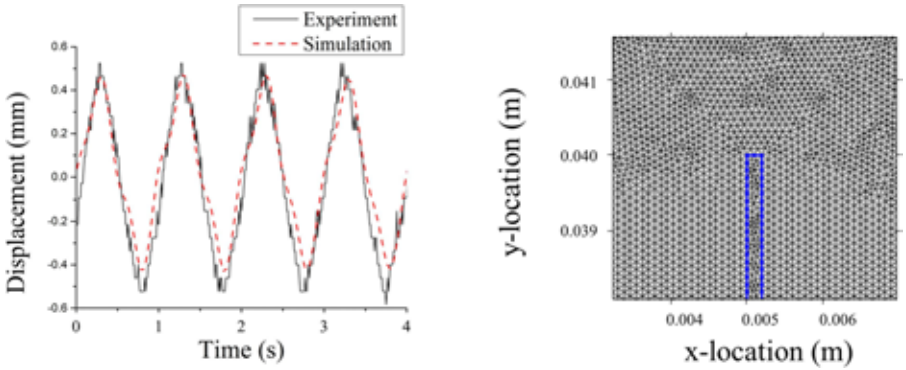

electrolyte-polymer interface. Table 3 provides the parameter values used in simulations.

Similar to conventional IPMC actuator modeling, a linear elastic material model with Newton's second law is utilized to solve deformation in the polymer fiber. With Newton's second law given as

$$\rho_p \frac{\partial^2 \boldsymbol{u}}{\partial t^2} - \nabla \cdot \sigma = \boldsymbol{F} \quad (3)$$

where ρ_p is the polymer density, $\boldsymbol{u}$ is the displacement vector, σ is the stress tensor, and $\boldsymbol{F}$ is the body force vector, where the component of $\boldsymbol{F}$ across the bending direction of the Nafion fiber is assumed to be proportional to the charge density within the polymer, that is

$$F_x = \alpha\rho \quad (4)$$

where α is the force-coupling coefficient, which is experimentally calibrated.

Simulation results for a 200-μm diameter, 40 mm long, EAP fiber submerged in LiCl electrolyte exposed to a 5-V, 1-Hz AC square wave, with 100 ×100 mm surface area electrodes spaced 10 mm apart, are shown in Figure 7. A comparison to experimental results is included for the same operating conditions. These results show good agreement with experimental data, indicating the model adequately captures the underlying actuation physics. Mesh refinement was performed up to 250,832 domain elements showing less than 2 % solution change. A close-up of the final utilized mesh at the free-end of the EAP fiber is shown in Figure 7.

Development of a Prototype Biomimetic Cilia Array

The fabricated cylindrical ionomer fibers were used as artificial cilia for designing a prototype cilia array. The biomimetic AM cilia array system was fabricated on a soft and flexible polydimethylsiloxane (PDMS) silicone elastomer substrate. The PDMS substrate was prepared using Sylgard® 184 silicone elastomer (Dow Corning). The PDMS prepolymer mixed at a 10:1 weight ratio of elastomer to hardener was cast into a mold and cured at room temperature for 48 h to obtain a flexible rubber-like substrate layer.

For accurate placement of cilia fibers, an array of holes with diameter of 50 μm was predrilled into the PDMS layer using a CNC milling machine. Figures 8a and 8b show microscopy images of the drilled holes. The melt-drawn ionomer microfibers were then planted into the PDMS substrate under a digital microscope using 29-gauge hypodermic needle. The process of fixing cilia fibers in the substrate is illustrated in Figures 8c, 8d, and 8e. First, a needle with an ionomer fiber was inserted along the predrilled hole and pushed slightly through the substrate. Then, the tip of the fiber was temporarily clamped while pulling out the needle, leaving the ionomer fiber securely fixed in a PDMS substrate. Figures 8f and 8g show the prototype AM cilia array system consisting of 20 fibers in row with 1-mm spacing in between. The diameter size of the fibers used in this prototype ranges from 70 to 90 μm, and free length is 8 mm. The substrate dimensions are 3.6 mm (W) × 2.4 mm (H) × 23 mm (L).

In order to actuate the AM cilia array by an external electric field, a

FIGURE 8

PDMS substrate with predrilled 50-µm holes for placement of EAP microfibers (a, b), process of fixing the ionomeric cilia fibers into a PDMS substrate (c, d, e), and digital optical microscope images of fabricated prototype AM cilia array with 1-mm spacing in between artificial cilia fibers (f, g).

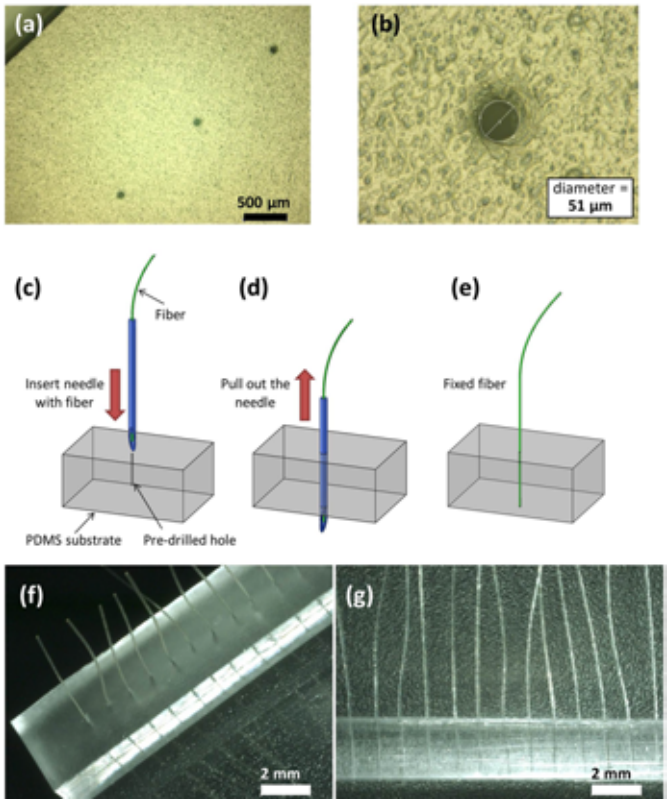

clamp device with six external electrodes was designed (Figure 9). The electrode assembly was fabricated from acrylic glass, and electrodes were made from Pt foil (thickness 0.001 in.). The clamp device consists of three sections (pairs) of electrodes that can be used to create a wave-like oscillation of cilia when sections are driven with phase difference. Figure 9b shows the prototype cilia fiber (1 × 20) array mounted between the electrodes and immersed in electrolyte solution. The electrodes shown are spaced 3.6 mm apart.

FIGURE 9

Clamp device with six external Pt electrodes for actuating the cilia (1 × 20) array by external field (a) and the artificial cilia array (1 × 20) mounted between electrodes and immersed in electrolyte solution (b).

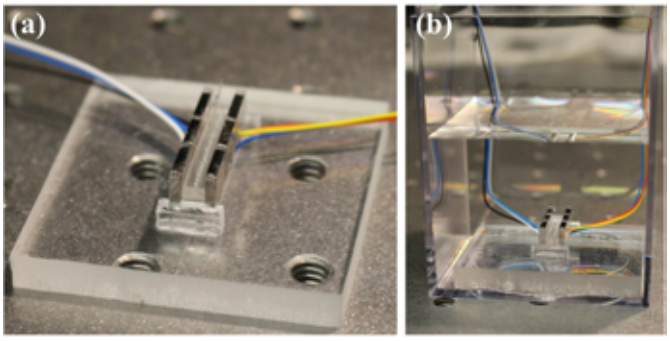

The prototype artificial cilia array was actuated by applying a 5-V AC, 0.5-Hz square wave input to alternating electrodes spaced 3.6 mm apart in a LiCl electrolyte solution. Video was collected at 30 frames per second. Tip displacement measurements were collected from the video at a rate of 10 Hz. The fibers show actuation displacements of several millimeters for the given case. Measured data and photographs from time of maximum displacements are shown in Figure 10.

Conclusions and Future Studies

The developed cilia-based microactuators are realizable and have been successfully implemented in a prototype microfiber array for prospective applications in underwater robotics and microfluidics. The microactuators can be wirelessly driven by low external electric field. They operate with low electronics requirements and can be designed as alternating actuators and sensors in different geometrical arrangements. Fabrication techniques as described are scalable up or down to meet desired design criteria. Application with microfibers acting as both sensors and actuators is being investigated for a full flow sensing and control system. This type of microarray device has many promising applications in microfluidics, robotics, and general marine operations. Problems such as accurate environmental sensing, *in situ* boundary layer and near-surface flow measurement, and chaotic or turbulent

FIGURE 10

Experimental results for a microfiber array actuated by separated electrodes at 5-V AC, 0.5-Hz square wave input applied to electrodes spaced 3.6 mm apart. Still photograph from video at times t = 1.3 s (a), t = 1.8 s (b), t = 2.3 s (c), t = 2.8 s (d), t = 3.3 s (e), t = 3.8 s (f), and measured tip displacement measurements of an individual fiber of the array (g).

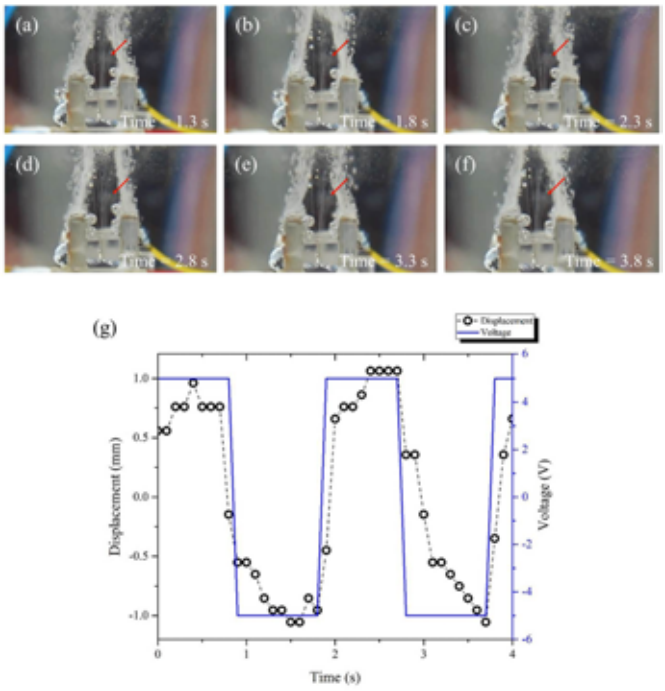

flow sensing and control can be addressed using this technology. This can be applied to underwater vehicles to improve handling and maneuverability, medical operations in cell and drug transport, and other capillary flow or microfluidic problems. Upon further development, this technology can play a significant role in achieving more advanced underwater robotic systems. The newly developed prototype AM array of microfibers presented above is crucial groundwork to further developments of active materials as employed in microfluidics and marine biomimetic studies.

Future work includes building an understanding for cilium motion and utilizing finite element modeling for design optimization. Further developments will be done in attempt to replicate similar motion to that of natural cilium. This can be expanded into arrays of cilia with phase shifts to move similarly to how systems of cilia move together. Natural cilia are able to produce consistent flow, locomotion, and organism displacement control. The ability to replicate natural cilia will benefit robotics, such as in biomimicry for artificial organs. Artificial cilia technologies of this type would be ideal for certain microfluidics, flow sensing and control systems, small organism locomotion, or similar application in biomedical devices.

Acknowledgments

This work was supported by the Office of Naval Research (N00014-13-1-0274). Special thanks go to Dr. Thomas McKenna.

Corresponding Author:

Kwang J. Kim
Active Materials and Smart Living Laboratory
Department of Mechanical Engineering, University of Nevada, Las Vegas (UNLV)
4505 S. Maryland Parkway,
Las Vegas, NV 89154
Email: kwang.kim@unlv.edu

References

Alici, G., Spinks, G.M., Madden, J.D., Wu, Y., & Wallace, G.G. 2008. Response characterization of electroactive polymers as mechanical sensors. IEEE/ASME T Mech. 13(2):187-96. http://dx.doi.org/10.1109/TMECH.2008.918531.

Ball, P. 1999. Engineering shark skin and other solutions. Nature. 400(6744):507-9. http://dx.doi.org/10.1038/22883.

Ball, P. 2001. Life's lessons in design. Nature. 409(6818):413-6. http://dx.doi.org/10.1038/35053198.

Ball, P. 2002. Natural strategies for the molecular engineer. Nanotechnology. 13(5):R15. http://dx.doi.org/10.1088/0957-4484/13/5/201.

Bandyopadhyay, P.R., Beal, D.N., & Menozzi, A. 2008. Biorobotic insights into how animals swim. J Exp Biol. 211(2):206-14. http://dx.doi.org/10.1242/jeb.012161.

Bar-Cohen, Y. 2004. Electroactive Polymer (EAP) Actuators as Artificial Muscles: Reality, Potential and Challenges, Second Edition. Bellingham, WA: SPIE Press. 816 pp. http://dx.doi.org/10.1117/3.547465.

Bar-Cohen, Y. 2006. Biomimetics? using nature to inspire human innovation. Bioinspir Biomim. 1(1):P1. http://dx.doi.org/10.1088/1748-3182/1/1/P01.

Bhushan, B. 2009. Biomimetics: lessons from nature–an overview. Philos T R Soc A. 367(1893):1445-86. http://dx.doi.org/10.1098/rsta.2009.0026.

den Toonder, J.M., & Onck, P.R. 2013. Microfluidic manipulation with artificial/bioinspired cilia. Trends Biotechnol. 31(2): 85-91. http://dx.doi.org/10.1016/j.tibtech.2012.11.005.

Deng, X., & Avadhanula, S. 2005. Biomimetic micro underwater vehicle with oscillating fin propulsion: system design and force measurement. In: Robotics and Automation, 2005. ICRA 2005. Proceedings of the 2005 IEEE International Conference. pp. 3312-7. Piscataway, NJ: IEEE.

Edd, J., Payen, S., Rubinsky, B., Stoller, M.L., & Sitti, M. 2003. Biomimetic propulsion for a swimming surgical micro-robot. In: Intelligent Robots and Systems, 2003. (IROS 2003). Proceedings. 2003 IEEE/RSJ International Conference. 3:2583-8. Piscataway, NJ: IEEE. http://dx.doi.org/10.1109/iros.2003.1249259.

Enuka, Y., Hanukoglu, I., Edelheit, O., Vaknine, H., & Hanukoglu, A. 2012. Epithelial sodium channels (ENaC) are uniformly distributed on motile cilia in the oviduct and the respiratory airways. Histochem Cell Biol. 137(3):339-53. http://dx.doi.org/10.1007/s00418-011-0904-1.

Feng, G.H., & Tsai, J.W. 2011. 3D omnidiectional contollable elastic IPMC tweezer with self-sensing and adjustable clamping force abilities for biomedical applications. In: Solid-State Sensors, Actuators and Microsystems Conference (TRANSDUCERS), 2011 16th International. pp. 1725-8. Piscataway, NJ: IEEE.

Fish, F.E., Howle, L.E., & Murray, M.M. 2008. Hydrodynamic flow control in marine mammals. Integr Comp Biol. 48(6):788-800. http://dx.doi.org/10.1093/icb/icn029.

Guo, S., Ge, Y., Li, L., & Liu, S. 2006. Underwater swimming micro robot using IPMC actuator. In: Mechatronics and Automation, Proceedings of the 2006 IEEE International Conference. pp. 249-54. Piscataway, NJ: IEEE. http://dx.doi.org/10.1109/icma.2006.257505.

Guo, S., Shi, L., Ye, X., & Li, L. 2007. A new jellyfish type of underwater microrobot. In: Mechatronics and Automation, 2007. ICMA 2007. International Conference. pp. 509-14. Piscataway, NJ: IEEE. http://dx.doi.org/10.1109/icma.2007.4303595.

Kamamichi, N., Yamakita, M., Asaka, K., & Luo, Z.W. 2006. A snake-like swimming robot using IPMC actuator/sensor. In: Robotics and Automation, 2006. ICRA 2006. Proceedings 2006 IEEE International Conference. pp. 1812-7. Piscataway, NJ: IEEE.

Kim, B., Kim, D.H., Jung, J., & Park, J.O. 2005. A biomimetic undulatory tadpole robot using ionic polymer-metal composite actuators. Smart Mater Struct. 14(6):1579. http://dx.doi.org/10.1088/0964-1726/14/6/051.

Kim, K.J., Yim, W., Paquette, J.W., & Kim, D. 2007. Ionic polymer-metal composites for underwater operation. J Intel Mat Syst Str. 18(2):123-31. http://dx.doi.org/10.1177/1045389X06063468.

Kim, K.J., Pugal, D., & Leang, K.K. 2011. A twistable ionic polymer-metal composite artificial muscle for marine applications. Mar Technol Soc J. 45(4):83-98. http://dx.doi.org/10.4031/MTSJ.45.4.9.

Kim, K.J., & Shahinpoor, M. 2003. Ionic polymer-metal composites: II. Manufacturing techniques. Smart Mater Struct. 12(1):65. http://dx.doi.org/10.1088/0964-1726/12/1/308.

Kim, K.J., Kim, S.J., & Wong, J. 2015. A novel fabrication process of multi degree of freedom (DOF) shaped electroactive polymer actuators/sensors for catheters. US Patent #9147825.

Ko, B.G., Kwon, H.C., & Lee, S.J. 2009. A self-sensing method for IPMC actuator. Adv Sci Tech. 56:111-5. http://dx.doi.org/10.4028/www.scientific.net/AST.56.111.

Kruusamäe, K., Brunetto, P., Graziani, S., Punning, A., Di Pasquale, G., & Aabloo, A. 2010. Self−sensing ionic polymer-metal composite actuating device with patterned surface electrodes. Polym Int. 59(3):300-4. http://dx.doi.org/10.1002/pi.2752.

Lauder, G.V., & Madden, P.G. 2007. Fish locomotion: kinematics and hydrodynamics of flexible foil-like fins. Exp Fluids. 43(5): 641-53. http://dx.doi.org/10.1007/s00348-007-0357-4.

Najem, J., Sarles, S.A., Akle, B., & Leo, D.J. 2012. Biomimetic jellyfish-inspired underwater vehicle actuated by ionic polymer metal composite actuators. Smart Mater Struct. 21(9):094026. http://dx.doi.org/10.1088/0964-1726/21/9/094026.

Oh, K., Chung, J.H., Devasia, S., & Riley, J.J. 2009. Bio-mimetic silicone cilia for microfluidic manipulation. Lab Chip. 9(11): 1561-6. http://dx.doi.org/10.1039/b817409a.

Palmre, V., Hubbard, J.J., Fleming, M., Pugal, D., Kim, S., Kim, K.J., & Leang, K.K.. 2012. An IPMC-enabled bio-inspired bending/twisting fin for underwater applications. Smart Mater Struct. 22(1):014003. http://dx.doi.org/10.1088/0964-1726/22/1/014003.

Pugal, D., Jung, K., Aabloo, A., & Kim, K.J. 2010. Ionic polymer-metal composite mechanoelectrical transduction: review and perspectives. Polym Int. 59(3): 279-89. http://dx.doi.org/10.1002/pi.2759.

Punning, A., Kruusamäe, M., & Aabloo, A. 2007. A self-sensing ion conducting polymer metal composite (IPMC) actuator. Sensor Actuat A-Phys. 136(2):656-64. http://dx.doi.org/10.1016/j.sna.2006.12.008.

Satir, P., & Christensen, S.T. 2007. Overview of structure and function of mammalian cilia. Annu Rev Physiol. 69:377-400. http://dx.doi.org/10.1146/annurev.physiol.69.040705.141236.

Satir, P., & Christensen, S.T. 2008. Structure and function of mammalian cilia. Histochem Cell Biol. 129(6):687-93. http://dx.doi.org/10.1007/s00418-008-0416-9.

Shahinpoor, M., & Kim, K.J. 2000. The effect of surface-electrode resistance on the performance of ionic polymer-metal composite (IPMC) artificial muscles. Smart Mater Struct. 9(4):543. http://dx.doi.org/10.1088/0964-1726/9/4/318.

Shahinpoor, M., & Kim, K.J. 2001. Ionic polymer-metal composites: I. Fundamentals.

Smart Mater Struct. 10(4):819. http://dx.doi.org/10.1088/0964-1726/10/4/327.

Shahinpoor, M., & Kim, K.J. 2004a. Ionic polymer-metal composites: III. Modeling and simulation as biomimetic sensors, actuators, transducers, and artificial muscles. Smart Mater Struct. 13(6):1362. http://dx.doi.org/10.1088/0964-1726/13/6/009.

Shahinpoor, M., & Kim, K.J. 2004b. Ionic polymer-metal composites: IV. Industrial and medical applications. Smart Mater Struct. 14(1):197. http://dx.doi.org/10.1088/0964-1726/14/1/020.

Shen, Q., Wang, T., Liang, J., & Wen, L. 2013. Hydrodynamic performance of a biomimetic robotic swimmer actuated by ionic polymer-metal composite. Smart Mater Struct. 22(7): 075035. http://dx.doi.org/10.1088/0964-1726/22/7/075035.

Shen, Q., Kim, K.J., & Wang, T. 2014. Electrode of ionic polymer-metal composite sensors: Modeling and experimental investigation. J Appl Phys. 115(19):194902. http://dx.doi.org/10.1063/1.4876255.

Shen, Q., Palmre, V., Stalbaum, T., & Kim, K.J. 2015. A comprehensive physics-based model encompassing variable surface resistance and underlying physics of ionic polymer-metal composite actuators. J Appl Phys. 118(12): 124904. http://dx.doi.org/10.1063/1.4931912.

Stalbaum, T., Pugal, D., Nelson, S.E., Palmre, V., & Kim, K.J. 2015. Physics-based modeling of mechano-electric transduction of tube-shaped ionic polymer-metal composite. J Appl Phys. 117(11):114903. http://dx.doi.org/10.1063/1.4914034.

Wen, L., Weaver, J.C., & Lauder, G.V. 2014. Biomimetic shark skin: design, fabrication and hydrodynamic function. J Exp Biol. 217(10):1656-6. http://dx.doi.org/10.1242/jeb.097097.

Yim, W., Lee, J., & Kim, K.J. 2007. An artificial muscle actuator for biomimetic underwater propulsors. Bioinspir Biomim. 2(2): S31. http://dx.doi.org/10.1088/1748-3182/2/2/S04.

Yu, J., Tan, M., Wang, S., & Chen, E. 2004. Development of a biomimetic robotic fish and its control algorithm. IEEE Sys Man Cybern. 34(4):1798-810. http://dx.doi.org/10.1109/TSMCB.2004.831151.

Zhang, W., Guo, S., & Asaka, K. 2006. Development of underwater microrobot with biomimetic locomotion. Appl Bionics Biomech. 3(3):245-52. http://dx.doi.org/10.1155/2006/395963.

Zhou, C., & Low, K.H. 2012. Design and locomotion control of a biomimetic underwater vehicle with fin propulsion. IEEE-ASME T Mech. 17(1):25-35. http://dx.doi.org/10.1109/TMECH.2011.2175004.

Zhou, Z.G., & Liu, Z.W. 2008. Biomimetic cilia based on MEMS technology. J Bionic Eng. 5(4):358-65. http://dx.doi.org/10.1016/S1672-6529(08)60181-X.